

# *Drosophila* Ryanodine Receptors Mediate General Anesthesia by Halothane

Shuying Gao, Ph.D.,\* David J. Sandstrom, Ph.D.,† Harold E. Smith, Ph.D.,‡ Brigit High, B.A.,§ Jon W. Marsh, Ph.D.,|| Howard A. Nash, M.D., Ph.D.##

## ABSTRACT

**Background:** Although *in vitro* studies have identified numerous possible targets, the molecules that mediate the *in vivo* effects of volatile anesthetics remain largely unknown. The mammalian ryanodine receptor (Ryr) is a known halothane target, and the authors hypothesized that it has a central role in anesthesia.

**Methods:** Gene function of the *Drosophila* Ryr (*dRyr*) was manipulated in the whole body or in specific tissues using a collection of mutants and transgenes, and responses to halothane were measured with a reactive climbing assay. Cellular responses to halothane were studied using  $\text{Ca}^{2+}$  imaging and patch clamp electrophysiology.

**Results:** Halothane potency strongly correlates with *dRyr* gene copy number, and missense mutations in regions known to be functionally important in the mammalian Ryrs gene cause dominant hypersensitivity. Tissue-specific manipulation of *dRyr* shows that expression in neurons and glia, but not muscle, mediates halothane sensitivity. In cultured cells, halothane-induced  $\text{Ca}^{2+}$  efflux is strictly *dRyr*-dependent, suggesting a close interaction between halothane and *dRyr*.  $\text{Ca}^{2+}$  imaging and electrophysiology of *Drosophila* central

## What We Already Know about This Topic

- Ryanodine receptors are involved in the pathogenesis of malignant hyperthermia, but their role in neurologic effects of anesthetics is less clear
- Model organisms provide a powerful genetics-based approach for studying anesthetic targets

## What This Article Tells Us That Is New

- Halothane immobilization of *Drosophila* flies was bidirectionally affected by mutations in the ryanodine receptor gene
- Immobilization required neurally expressed ryanodine receptors and halothane increased intracellular calcium, a mechanism that might also be relevant to anesthetic actions in vertebrates

neurons reveal halothane-induced  $\text{Ca}^{2+}$  flux that is altered in *dRyr* mutants and correlates with strong hyperpolarization.

**Conclusions:** In *Drosophila*, neurally expressed *dRyr* mediates a substantial proportion of the anesthetic effects of halothane *in vivo*, is potently activated by halothane *in vitro*, and activates an inhibitory conductance. The authors' results provide support for Ryr as an important mediator of immobilization by volatile anesthetics.

**V**OLATILE general anesthetics are simple organic compounds that rapidly and reversibly suppress responsiveness to external stimuli in all animals while leaving basal functions intact. These properties have rendered anesthetics indispensable in the clinic and made them attractive tools for studying the control of arousal. One obstacle to progress is that, despite considerable effort over many years, the molecular pathways through which volatile anesthetics act remain largely unknown. *In vitro* studies have identified many proteins whose activity is affected by clinical concentrations of volatile general anesthetics,<sup>1</sup> but validating these candidates *in vivo* has proven difficult.

Studies in genetic model organisms such as worms, flies, and mice have been instrumental in identifying novel targets of volatile anesthetics and have provided *in vivo* validation of candidates identified *in vitro*.<sup>2-6</sup> These mutants illustrate several features of the molecular pathways mediating anesthesia. First, voltage-insensitive ("leak") ion channels, which act to hyperpolarize neurons, have repeatedly appeared in genetic screens for targets of volatile anesthetics,<sup>2,3,5,7</sup> suggesting that they act, at least in part, through changes in voltage

\* Postdoctoral Research Fellow, Laboratory of Molecular Biology, † Staff Scientist, Laboratory of Molecular Biology, National Institute of Mental Health, ‡ Staff Scientist, Genomics Core, National Institute of Diabetes, Digestive and Kidney Disease, National Institutes of Health, Bethesda, Maryland. § Undergraduate Intern, Laboratory of Molecular Biology. Current position: National Institute of Neurological Disorders and Stroke, National Institutes of Health. || Staff Scientist, Laboratory of Cellular and Molecular Regulation, National Institute of Mental Health. ## Senior Investigator, Laboratory of Molecular Biology, National Institutes of Health.

Received from the Laboratory of Molecular Biology, National Institute of Mental Health, National Institutes of Health. Submitted for publication March 20, 2012. Accepted for publication November 1, 2012. Supported by the National Institute of Mental Health, Division of Intramural Research, National Institutes of Health, Department of Health and Human Services, Bethesda, Maryland. Drs. Gao and Sandstrom contributed equally to this work.

Address correspondence to Dr. Sandstrom: Biological Sciences Program, University of Maryland College Park, The Universities at Shady Grove Campus, 9630 Gudelsky Drive, Building 2, Room 4092, Rockville, MD 20850. sandstrd@umd.edu. Information on purchasing reprints may be found at [www.anesthesiology.org](http://www.anesthesiology.org) or on the masthead page at the beginning of this issue. ANESTHESIOLOGY's articles are made freely accessible to all readers, for personal use only, 6 months from the cover date of the issue.

Copyright © 2013, the American Society of Anesthesiologists, Inc. Lippincott Williams & Wilkins. Anesthesiology 2013; 118:587-601

and resistance across the plasma membrane. Second, the response to each anesthetic compound is affected differently by a given mutant, suggesting the presence of agent-specific pathways.<sup>2,8</sup> Finally, mutations in these genes reduce but do not eliminate sensitivity to volatile anesthetics, indicating that additional anesthetic targets remain unidentified.

The ryanodine receptor (Ryr), a large-conductance channel that mediates release of  $\text{Ca}^{2+}$  from internal stores, is known to be activated by volatile anesthetics, especially halothane.<sup>9,10</sup> However, the study of the interaction between halothane and Ryr has been largely limited to muscle, where halothane potently induces malignant hyperthermia, a pathologic condition defined by inappropriate activation of Ryr in susceptible humans and swine.<sup>11</sup> Despite the clear connection between Ryr and halothane, the role of neurally expressed Ryr in the immobilizing effects of halothane is unexplored.

In this study, we use *Drosophila* genetics to test the hypothesis that Ryr mediates halothane anesthesia. We find that dRyr is a major determinant of halothane's anesthetic effects in flies and that these effects are mediated by expression of dRyr in the nervous system, but not muscle.

## Materials and Methods

### Fly Stocks and Genetic Analysis

All flies were reared on cornmeal-molasses medium and maintained at 25°C in a 12-h light–dark cycle. The following fly strains were used in this study: *dRyr*<sup>k04913</sup>, *Appl-GAL4*, *nrv2-GAL4*, *cn<sup>1</sup> l(2)44Fp<sup>1</sup> bw<sup>1</sup> sp<sup>1</sup>/SM6a*, *cn<sup>1</sup> l(2)44F<sup>1</sup> bw<sup>1</sup> sp<sup>1</sup>/SM6a*, *l(2)44Fa<sup>3</sup>/CyO*, *l(2)44Ff<sup>1</sup>/CyO*, *l(2)44Fg<sup>1</sup>/CyO*, *l(2)44Fh<sup>1</sup>/CyO*, and *l(2)44Fj<sup>1</sup>/CyO* (*Drosophila* Stock Center, Bloomington, IN); *dRyr*<sup>GS21220</sup> (*Drosophila* Genetic Resource Center, Kyoto, Japan); and *UAS-dRyr*<sup>RNAi</sup> (10844R-3, National Institute of Genetics, Japan). *UAS-GCaMP3* was a generous gift from the Howard Hughes Medical Institute (Janelia Farm, Ashburn, VA); *elav-GAL4* was a generous gift from Ravi Allada, Ph.D. (Professor, University of Chicago, Chicago, IL); *repo-GAL4* was from Chi-Hon Lee, Ph.D. (Senior Investigator, National Institute of Child Health and Human Development, Bethesda, MD); *MHC-GAL4* was from Benjamin White, Ph.D. (Senior Investigator, National Institute of Mental Health, Bethesda, MD); and *ShakB-GAL4* and *Canton-S* were from the lab stock collection. *dRyr*<sup>k04913</sup>, *dRyr*<sup>GS21220</sup>, *dRyr*<sup>Δ25</sup>, *elav-GAL4*, *nrv2-GAL4*, and *UAS-dRyr*<sup>RNAi</sup> were made congenic with *Canton-S* by outcrossing for seven generations. As described previously,<sup>12</sup> *dRyr*<sup>k04913</sup> was homozygous lethal. However, the lethality was not rescued by the genomic duplication *dRyr*<sup>24D03</sup>, indicating that it resulted from a closely linked mutation outside the *dRyr* locus.

Behavioral assays of anesthesia are subject to a number of confounding factors, including genetic background and subtle environmental variations. To avoid such confounding factors, all comparisons were made within experiments run in parallel over the same time and only between groups matched for genetic background.

The deletion mutant *dRyr*<sup>Δ25</sup> was generated by excising the region between transposons *P{XP}d03686* and *P{XP}d03830* (Exelixis Stock Collection, Boston, MA), using flippase-mediated recombination at flippase recombination target sites present in these elements.<sup>13</sup> The deletion was verified using polymerase chain reaction amplification and DNA sequencing.

The genomic duplication *dRyr*<sup>24D03</sup> was generated by integrating the P[acman] clone CH321-24D03 (Bellen Laboratory, Baylor College of Medicine, Houston, TX) into the VK33 docking site on the third chromosome *via* ΦC31-mediated site-specific integration.<sup>14</sup> *UAS-dRyr-V5* was generated by cloning a 15.6-kb PacI-PsiI fragment from DRyR-15B (kindly provided by Daniel Cordova, M.Sc., Senior Biochemist, Dupont Crop Protection, Newark, DE) into the pUAST vector, and injecting the construct into *Canton-S* flies that carried the *w*<sup>1118</sup> mutation. All injections were performed by Rainbow Transgenic Flies, Inc. (Camarillo, CA).

### Genomic Sequencing to Identify dRyr Mutation Sites

The genomic DNA libraries from both control and mutant strains used in this study were constructed and sequenced in accordance with the manufacturer's protocols (Illumina, San Diego, CA). Briefly, 1 μg of genomic DNA was sheared by sonication, end-repaired, A-tailed, adapter-ligated, size-fractionated by gel electrophoresis, and amplified by polymerase chain reaction. Paired-end 101-cycle sequencing on a HiSeq 2000 instrument (Illumina) yielded an average of 20 million reads (range, 13–30 million reads) equivalent to approximately 29-fold coverage (range, 19- to 43-fold). Reads were aligned to the *Drosophila melanogaster* reference genome (dm3; Berkeley *Drosophila* Genome Project Release 5) with BFAST.<sup>15</sup> SAMTools<sup>16</sup> was used to call sequence variants, and nonsynonymous mutations were identified using ANNOVAR.<sup>17</sup>

To generate a list of unique candidate mutations, we filtered sequence variants in the mutant strains against those present in the control strain. This process revealed that only *dRyr* contained sequence variants in all of the *dRyr* alleles carrying the ethylmethanesulfonate mutations. Pairwise alignments were carried out with mammalian Ryr isoforms using BLASTP.

### Tissue Homogenates and Western Blots

After flies were tested in the reactive climbing assay, 200 fly heads or 50–100 whole flies from each genotype were used to prepare homogenates. The samples were homogenized in 100–200 μl of homogenization buffer (0.25 M sucrose, 10 mM Tris, and 1 mM EDTA) and protease inhibitors (Roche, Indianapolis, IN). The homogenates were centrifuged for 10 min at 1,000g at 4°C. The supernatant was centrifuged again for 40 min at 48,000g at 4°C to extract membrane protein. The pellet was resuspended (50 mM Tris [pH 7.4], 150 mM NaCl, 1 mM EDTA, and protease inhibitors), and 20 to 30 μg of protein was processed, electrophoresed, and

transferred according to the supplier's instructions (Invitrogen, Carlsbad, CA). Blots were probed with anti-dRyr (rabbit polyclonal, a generous gift from Daniel Cordova, M.Sc., Senior Biochemist, Dupont Crop Protection) at a 1:1,000 dilution, and anti-Na,K-ATPase (mouse mAb $\alpha$ 5; Developmental Studies Hybridoma Bank, Iowa City, IA) at 1.3 ng/ml. Secondary antibodies were peroxidase-linked and used according to the supplier's instructions. Blots were developed with the enhanced chemiluminescence detection system (GE Healthcare, Piscataway, NJ). For quantification, four independent homogenates were prepared for each genotype, and two aliquots of each were analyzed, yielding eight blots for each genotype. Intensities of dRyr bands were measured and normalized to those of Na,K-ATPase using ImageJ (National Institutes of Health, Bethesda, MD).

### Reactive Climbing Assay

The reactive climbing assay, also known as the distribution test, was performed as described previously.<sup>18</sup> Male flies aged 3–7 days were collected and sorted under carbon dioxide anesthesia and allowed to recover for 1 day. Without further anesthesia, flies were loaded into testing vials (10 per vial), consisting of 50-ml tubes perforated to allow gas exchange. Testing vials were equilibrated in a chamber with a constant flow of a fixed concentration of volatile anesthetics—halothane (Sigma, St. Louis, MO), sevoflurane and enflurane (RxElite, Boise, ID), and isoflurane (Baxter Healthcare, Deerfield, IL)—for 35–45 min. After equilibration, the flies were tapped down quickly to the bottom of the vial several times at 30-s intervals. After the last round of tapping, the flies were allowed to climb for 1 min, after which the proportion remaining at the conical bottom of the testing vial (fraction down) was recorded. Flies were tested with three or four more concentrations of anesthetic, progressively increased by 0.05% with each successive test, and equilibrated for 35–45 min before each test. Naive flies of the same genotype were then tested at the four or five higher concentrations to produce the full concentration–response curve of 8–10 concentrations, covering the full range from 0% down to 100% down. The process was repeated twice with naive flies. In total, this yielded a sample size of nine for each combination of drug and genotype.

### Countercurrent Locomotion Assay

The countercurrent assay was performed as described previously.<sup>19</sup> Typically, a group of 30 male flies of each genotype, aged 3–7 days, were loaded into the start tube, tapped to the bottom, and given 10 s to climb up into a transfer tube at top. The flies in each transfer tube were then shifted into the next base tube by banging the device. This was repeated four more times at 10-s intervals, and at the end, the flies in each base tube were counted. A transfer probability,  $P_t$ , is calculated by the following formula:  $P_t = [n \times (\text{no. of flies in the base tube } n)] / 5 \times (\text{no. of flies in all tubes})$ . The experiment was performed three to five times for each genotype.

### Sf9 Cell Culture and Flow Cytometry

Sf9 cells stably transfected with dRyr<sup>20</sup> were a generous gift from Daniel Cordova, M.Sc. Wild-type Sf9 cells were purchased from Invitrogen. Cultures were maintained at 28°C in SF900-II serum-free medium (Invitrogen), without antibiotics, and subcultured at confluence by sloughing, approximately twice weekly.

To prepare Sf9 cells for Ca<sup>2+</sup> imaging, they were suspended, centrifuged, washed in Ca<sup>2+</sup> imaging saline (130 mM NaCl, 5.4 mM KCl, 1.2 mM MgCl<sub>2</sub>, 1 mM CaCl<sub>2</sub>, 4.2 mM NaHCO<sub>3</sub>, 7.3 mM NaH<sub>2</sub>PO<sub>4</sub>, 10 mM glucose, and 63 mM sucrose),<sup>20</sup> and then centrifuged and resuspended in 5 ml of Ca<sup>2+</sup> imaging saline containing 1  $\mu$ M of the acetoxymethyl ester of a Fluo Calcium indicator (Fluo-5N AM in most experiments) plus Pluronic F-127 (Invitrogen). Cells were incubated in Fluo-acetoxymethyl for 30–45 min, and then washed in Ca<sup>2+</sup> imaging saline for a minimum of 30 min before cytometry. Aliquots containing approximately  $0.5 \times 10^6$  cells were placed in styrene tubes and treated with anesthetics and/or thapsigargin (Tocris Bioscience, Minneapolis, MN), and fluorescence of the Fluo indicator was measured on a BD FACScan (Becton-Dickinson, Franklin Lakes, NJ). Debris and dead cells were gated out by size and fluorescence caused by propidium iodide uptake, respectively. Intracellular Ca<sup>2+</sup> concentration was calibrated at the end of the experiment by sequential addition of ionomycin (Tocris) and EGTA, calculated as described by Tsien *et al.*,<sup>21</sup> using  $K_d = 2.3 \mu\text{M}$  for Fluo-5F and 90  $\mu\text{M}$  for Fluo-5N. Offline analysis of cytometry data was carried out using Flow-Jo 7.6.1 (Tree Star, Inc., Ashland, OR). Anesthetic concentrations in solution were converted to partial atmospheric pressures using Ostwald water/gas partition coefficients.

### Ca<sup>2+</sup> Imaging in Larval Central Nervous System

Changes in internal Ca<sup>2+</sup> were visualized in the cell body of motoneuron RP2 (MNISN1s) using the genetically encoded Ca<sup>2+</sup> indicator GCaMP3<sup>22</sup> driven by *ShakB-GAL4*. The central nervous system was dissected from the larva, and brain lobes were removed and mounted dorsal side down on a polyornithine-coated 25-mm coverslip, which formed the bottom of the recording chamber (Warner Instruments, Hamden, CT), mounted in a custom-fabricated plate that fit into the stage of a Nikon C-1 inverted confocal microscope (Nikon Instruments, Tokyo, Japan). This setup allowed for superfusion from above, and the preparation was imaged using a 60 $\times$  oil immersion objective from below. The preparation was scanned at 1 Hz, with the laser at minimum power and the pinhole opened to 100  $\mu\text{m}$ .

Recording solution (70 mM NaCl, 5 mM KCl, 0.3 mM CaCl<sub>2</sub>, 4 mM MgCl<sub>2</sub>, 10 mM NaHCO<sub>3</sub>, 5 mM trehalose, 115 mM sucrose, 5 mM HEPES, pH 7.2)<sup>23</sup> was perfused at 2 ml/min using a peristaltic pump, with solutions selected *via* remote-controlled solenoid valve. Anesthetics were vortexed into solution for 1–2 min and perfused from sealed reservoirs. Concentrations of anesthetic in contact with cells were



determined *via* head-space analysis of 50- $\mu$ l samples of solutions collected from the chamber, using an Agilent 6850 gas chromatograph.<sup>24,25</sup>  $\text{Ca}^{2+}$  imaging data were analyzed using Nikon EZ-C1 software. Because of their superficial positions, RP2s in multiple segments could be visualized at once, allowing analysis of four to eight cells per preparation. The entire cell body of each cell in the focal plane of a given preparation was defined as a region of interest, and the average pixel intensity *versus* time was determined. Because the background signal in regions outside of RP2 somata was essentially nil, background subtraction was unnecessary.  $\Delta F/F$  was calculated by dividing the intensity at a given time by the average of samples 1–10, subtracting 1 to set the initial value to 0, and multiplying by 100 to generate a percentage change.

### Electrophysiology

Whole-cell recordings were performed largely as described previously.<sup>24</sup> The external solution was identical (118 mM NaCl, 2 mM NaOH, 2 mM KCl, 4 mM  $\text{MgCl}_2$ , 0.5 mM  $\text{CaCl}_2$ , 60 mM sucrose, 5 mM trehalose, 5 mM HEPES, pH 7.1, 300–305 mOsm/kg). The internal solution differed by the addition of Mg-ATP and GTP-Tris (152 mM potassium gluconate, 2 mM NaCl, 0.1 mM  $\text{CaCl}_2$ , 10 mM HEPES, 1 mM EGTA, 4 mM Mg-ATP, 0.6 mM GTP-Tris, 8.4 mM KOH, pH 7.2, 290–295 mOsm/kg). A larval central nervous system, expressing *UAS-mcd8-GFP* in RP2 under the control of *ShakB-GAL4*, was mounted on a polyornithine-coated chip of coverslip. The region of the sheath around RP2 somata in segment A5 was softened with collagenase type XIV (Sigma) and removed manually with a suction pipette. Gigaseals were formed under the guidance of Nomarski optics, and membrane voltage was recorded using an AxoPatch 200B (Axon Instruments, Union City, CA) in current clamp mode. Recording parameters and solutions were controlled, and data were recorded using pClamp 8 (Axon). Drugs were dissolved as described above under  $\text{Ca}^{2+}$  Imaging in Larval Central Nervous System and perfused at 2 ml/min.

### Statistical Analysis

Reactive climbing data were analyzed largely as described previously.<sup>18</sup> In brief, the data were entered into SPSS 13 (SPSS Inc., Chicago, IL) and fitted with the concentration–response relationship: fraction down =  $C^n / (C^n + \text{EC}_{50}^n)$ , using logit analysis,<sup>26,27</sup> where  $C$  is the anesthetic concentration,  $n$  reflects the steepness of the curve and is shared between genotypes for each experiment, and  $\text{EC}_{50}$  is the anesthetic concentration at the midpoint of the curve. Each vial of flies was used for four to five anesthetic concentrations, so that the full range of eight concentrations required a pair of vials. The  $\text{EC}_{50}$  was determined for each pair of vials, for which the percentage shift in  $\text{EC}_{50}$  was derived using the following formula:

$$\% \text{shift in } \text{EC}_{50} = 100 \times \left\{ \frac{[\text{EC}_{50} (\text{experimental}) - \text{EC}_{50} (\text{control})]}{\text{EC}_{50} (\text{control})} \right\} \quad (1)$$

Flow cytometry and GCaMP3 fluorescence data were analyzed statistically in SigmaPlot 11.0 (Systat Software, Inc., San Jose, CA). For fitting of concentration–response curves for Fluo-5 fluorescence, data were normalized by defining percentage of untreated cells with elevated  $[\text{Ca}^{2+}]_i$  as 0 and those treated with saturating concentrations of anesthetic as 1, and the resulting relationships were fitted with a three-parameter Hill equation. Concentration–response curves for GCaMP3 fluorescence were plotted and analyzed as for Fluo-5, but using  $\Delta F/F$  values. A few preparations that responded with exaggerated  $\text{Ca}^{2+}$  flux to halothane concentrations above 2.0 mM were excluded from the concentration–response analysis by Dixon's test for outliers.

All data fit the assumptions for parametric statistics. Differences between two groups were assessed using the Student  $t$  test. Comparisons involving a single factor were performed using one-way ANOVA. The analysis of multiple genotypes and anesthetics described below under *dRyr* Mutations Have Weaker Effects on Other Volatile Anesthetics was performed with two-way ANOVA. The Bonferroni–Dunn test was used for *post hoc* analysis. Because of the conservative nature of the Bonferroni correction,  $P$  values were equal to 1 in a small number of cases.

## Results

### Ryanodine Receptor Insertion Mutants Are Resistant to Halothane

The *Drosophila* genome contains a single *Ryr* gene at cyto-logic position 44F.<sup>12,28</sup> In our initial tests of the role of *dRyr* in the response to the volatile anesthetic halothane, we used *dRyr*<sup>*k04913*</sup>, a hypomorphic mutant allele resulting from the insertion of a transposon 399 bases upstream of the start codon of *dRyr*,<sup>12</sup> and *dRyr*<sup>*GS21220*</sup>, nine bases upstream of *dRyr*<sup>*k04913*</sup> (fig. 1A). *dRyr*<sup>*GS21220*</sup> is homozygous viable, whereas, as described previously,<sup>12</sup> *dRyr*<sup>*k04913*</sup> is lethal, presumably because of a tightly linked mutation outside the *dRyr* locus (see above under Materials and Methods for details). Given the close proximity of the transposons in the two alleles, we expected them to produce similar phenotypes.

We examined the response of the mutants to halothane using a reactive climbing assay that evaluates the flies' righting/climbing reflex following mechanical agitation in the presence of anesthetic.<sup>18</sup> Under these conditions, wild-type *Canton-S* male flies exhibited a halothane-dependent decrease in locomotor activity, resulting in an increase in the proportion failing to climb ("Fraction Down"; fig. 1B, black curve), with flies lying immobile at the bottom of the vial at the highest anesthetic concentrations. For heterozygous *dRyr*<sup>*GS21220*</sup>/+ and *dRyr*<sup>*k04913*</sup>/+, and the transheterozygote *dRyr*<sup>*k04913*</sup>/*dRyr*<sup>*GS21220*</sup>, the concentration–response curves shifted to the right, indicating resistance to halothane relative to the wild-type. The effective concentrations (vol/vol) at which 50% of flies were down ( $\text{EC}_{50}$ ) were 0.22%, 0.22%, and 0.27% for *dRyr*<sup>*GS21220*</sup>/+, *dRyr*<sup>*k04913*</sup>/+, and

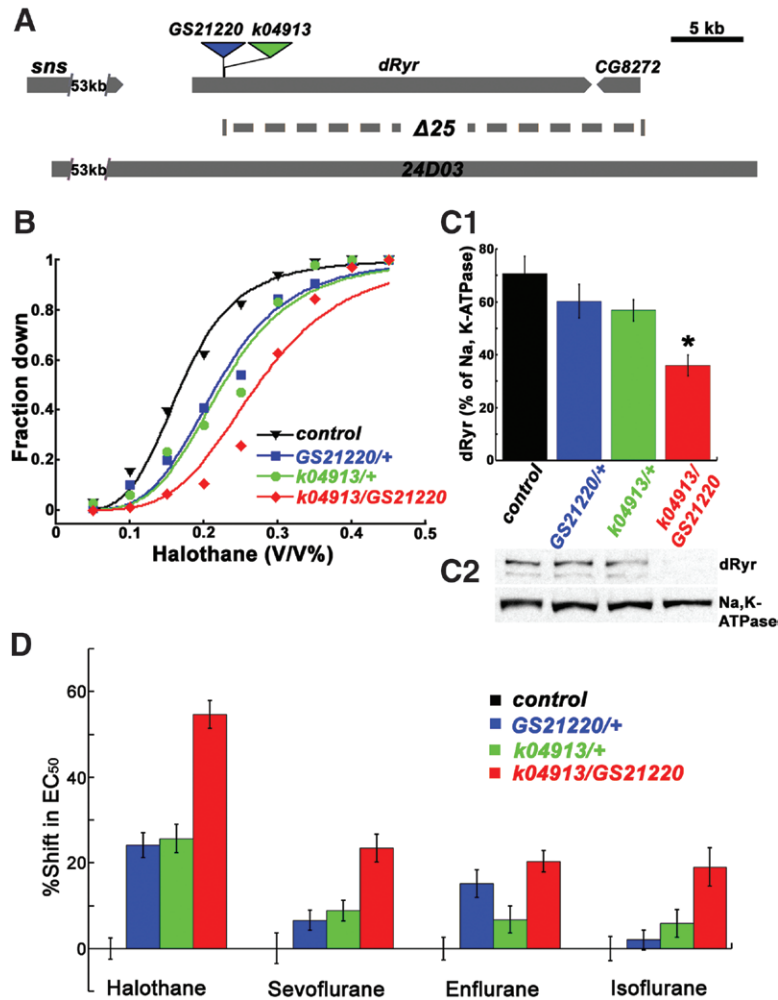


**Fig. 1.** *dRyr* mutants display preferential resistance to halothane. (A) Genetic map of *dRyr* region. The insertion sites of *dRyr*<sup>GS21220</sup> (blue triangle) and *dRyr*<sup>k04913</sup> (green triangle) are diagrammed above the genomic structure. The dashed line below the *dRyr* gene indicates the genomic segment deleted in *dRyr*<sup>Δ25</sup>. The genomic extent of CH321-24D03, which was used to generate the duplication strain *dRyr*<sup>24D03</sup>, is represented by the gray bar at the bottom. (B) *dRyr* mutants show resistance to the volatile anesthetic halothane in the reactive climbing assay. Canton-S flies (control, black triangles) respond to halothane in a concentration-dependent fashion (solid line is a fit of the data in the logit model). The concentration-response curves of *dRyr*<sup>GS21220/+</sup> (blue squares) and *dRyr*<sup>k04913/+</sup> (green circles) shift to the right relative to the control, indicating increased resistance. *dRyr*<sup>k04913/dRyr</sup><sup>GS21220</sup> (red diamonds) shows an even stronger halothane resistance. (C) *dRyr* protein expression is decreased in *dRyr* mutants. (C1) Quantification of *dRyr*, normalized to Na,K-ATPase. Values are mean ± SEM, with statistical significance indicated by an asterisk (\**P* = 0.0005) (*n* = 8). (C2) A representative Western blot. (D) *dRyr* mutants affect halothane anesthesia in preference to the effects of other anesthetics. Data are plotted as the shift in EC<sub>50</sub>, the concentration at which half of the flies are down, compared to the wild-type. *dRyr* mutants, *dRyr*<sup>GS21220/+</sup> (blue); *dRyr*<sup>k04913/+</sup> (green); and *dRyr*<sup>k04913/dRyr</sup><sup>GS21220</sup> (red) have a strong effect on halothane sensitivity and a weak effect on the sensitivity to sevoflurane, enflurane, and isoflurane. Detailed comparisons are described in the Results section. Values are mean ± SEM. *dRyr* = *Drosophila Ryr*.

*dRyr*<sup>k04913/dRyr</sup><sup>GS21220</sup>, respectively, all of which were significantly higher than that of the wild-type control (0.17% vol/vol; fig. 1B; *P* < 0.0001 for all, two-way ANOVA and Bonferroni-Dunn *post hoc* tests). In separate experiments, the EC<sub>50</sub> for *dRyr*<sup>GS21220</sup> homozygotes (0.27%) was also significantly higher than for matched controls (0.20%; *P* < 0.0001, Student *t* test).

Reduction in halothane sensitivity was paralleled by reduction in *dRyr* protein levels (fig. 1C). There was a significant effect of genotype on protein levels (*P* = 0.0009,

one-way ANOVA), and the allelic combination that reduced halothane sensitivity the most, *dRyr*<sup>k04913/dRyr</sup><sup>GS21220</sup>, reduced *dRyr* protein levels significantly. *dRyr* protein levels in the heterozygotes were intermediate between the wild-type and *dRyr*<sup>k04913/dRyr</sup><sup>GS21220</sup>, but Bonferroni-Dunn *post hoc* tests failed to demonstrate significant differences from control. We conclude that the insertion alleles reduce *dRyr* expression, but that anesthetic sensitivity discriminates between alleles more effectively than do immunoblots.

### *dRyr* Mutations Have Weaker Effects on Other Volatile Anesthetics

Previous work identified target genes for anesthetic action that have a distinct preference for halothane over other anesthetic agents, implying the presence of agent-specific pathways.<sup>2,8</sup> To determine the level of anesthetic specificity of *dRyr*, we assayed the responses of *dRyr* mutants to sevoflurane, enflurane, and isoflurane, and compared them to the response to halothane using a two-way ANOVA (generalized linear model; fig. 1D). There was a significant effect of anesthetic agent on the magnitude of shifts in  $EC_{50}$ , with halothane having the strongest effect ( $P < 0.0001$ , two-way ANOVA). In Bonferroni–Dunn *post hoc* tests, *dRyr*<sup>k04913</sup>/*dRyr*<sup>GS21220</sup> mutants were resistant to sevoflurane, enflurane, and isoflurane compared with wild-type controls. *dRyr*<sup>k04913</sup>/+ produced small shifts in the  $EC_{50}$  values for sevoflurane, enflurane, and isoflurane that were not significantly different

from wild-type controls, and were significantly smaller than the effect of this allele on halothane. *dRyr*<sup>GS21220</sup>/+ had mixed effects. It showed significant resistance to enflurane, which was not significantly different from that for halothane, but did not significantly affect the response to sevoflurane or isoflurane. *dRyr* mutants were therefore more resistant to the anesthetic effects of halothane than to those of other volatile agents, implicating *dRyr* as a component of the pathway(s) that regulates halothane sensitivity.

### Halothane Sensitivity Correlates with *dRyr* Copy Number

To explore the relationship between *dRyr* gene copy number, *dRyr* protein levels, and halothane sensitivity more systematically, we generated flies with the *dRyr* gene deleted or duplicated. The deletion *dRyr*<sup>Δ25</sup> was created by excising the region between two transposable elements using flippase–flippase recombination target-mediated recombination (fig. 1A). The

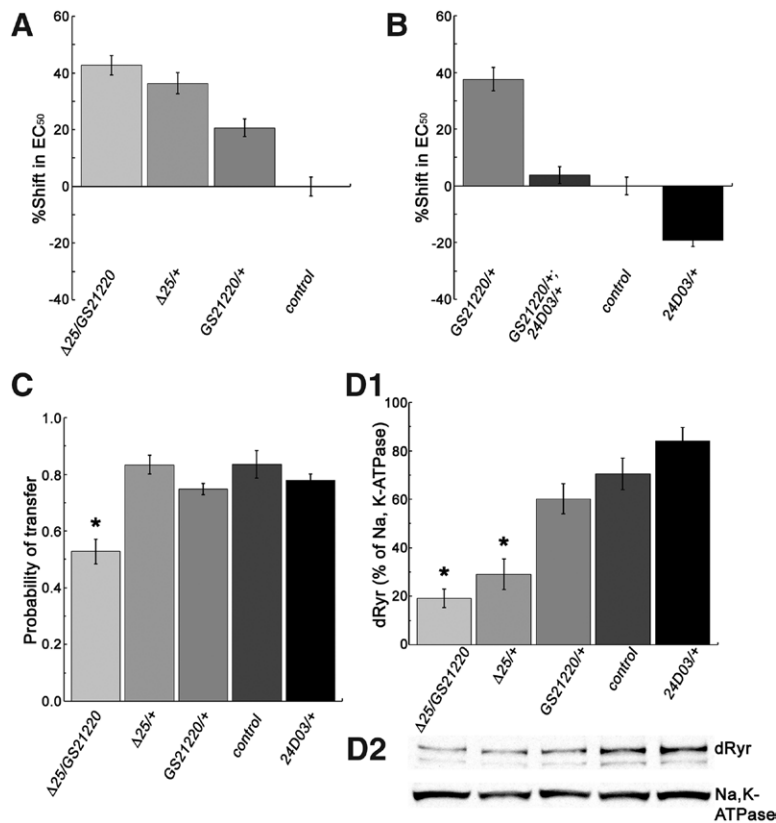


**Fig. 2.** Sensitivity to halothane follows *dRyr* copy number. (A) Reduced *dRyr* copy number is associated with resistance to halothane. Heterozygous *dRyr* deletion mutant *dRyr*<sup>Δ25</sup>/+ (medium gray), carrying one copy of *dRyr*, is resistant to halothane compared with the control, *Canton-S*, which carries two copies. *dRyr*<sup>Δ25</sup>/*dRyr*<sup>GS21220</sup> transheterozygotes (light gray) are resistant compared with the wild-type and *dRyr*<sup>GS21220</sup>/+ (dark gray). (B) The *dRyr* duplication strain *dRyr*<sup>24D03</sup>/+ (black), carrying three copies of *dRyr*, is more sensitive to halothane than its control (VK33 without insertion, carrying two copies of *dRyr*). Introducing *dRyr*<sup>24D03</sup> into insertion mutant *dRyr*<sup>GS21220</sup> (*dRyr*<sup>GS21220</sup>/+; *dRyr*<sup>24D03</sup>/+, dark gray) rescues the resistant phenotype of *dRyr*<sup>GS21220</sup>/+ (gray) to normal levels. Values are mean  $\pm$  SEM. (C) In the absence of anesthetic *dRyr*<sup>Δ25</sup>/+ (gray), *dRyr*<sup>GS21220</sup>/+ (dark gray), and *dRyr*<sup>24D03</sup> (black) display normal locomotor activity, whereas *dRyr*<sup>Δ25</sup>/*dRyr*<sup>GS21220</sup> (light gray) is significantly less active than control flies. Values are mean  $\pm$  SEM ( $n = 3-5$ ), and the asterisk denotes statistical significance ( $P = 0.0006$ , one-way ANOVA and Bonferroni–Dunn *post hoc* tests). (D) *dRyr* copy number affects *dRyr* protein expression. (D1) Quantification of *dRyr* protein levels. Asterisks denote statistically significant difference from the wild-type ( $P < 0.0001$  and  $P < 0.0001$ , one-way ANOVA and Bonferroni–Dunn *post hoc* tests). Values are mean  $\pm$  SEM ( $n = 8$ ). (D2) A representative Western blot, showing trend of increasing *dRyr* expression with the number of *dRyr* copies. *dRyr* = *Drosophila Ryr*.

resulting lethal allele removes all but the first exon of *dRyr* and all of *CG8272*, a gene of unknown function. This allele produces significant resistance to halothane, both in a heterozygous state and in combination with the hypomorphic allele *Ryr<sup>GS21220</sup>* (fig. 2A;  $P < 0.0001$  and  $P < 0.0001$ , one-way ANOVA and Bonferroni–Dunn *post hoc* tests). In *dRyr<sup>A25</sup>/+* animals, which possess exactly one copy of *dRyr*, halothane  $EC_{50}$  is 36% higher than in wild-type controls. Transheterozygous *dRyr<sup>A25</sup>/dRyr<sup>GS21220</sup>* mutants shift halothane  $EC_{50}$  by 43% (fig. 2A), which is significantly higher than the wild-type but not different from *dRyr<sup>A25</sup>/+*. As might be expected for a hypomorphic mutation, *dRyr<sup>GS21220</sup>/+* had intermediate effects, significantly higher than the wild-type and lower than *dRyr<sup>A25</sup>/+* or *dRyr<sup>A25</sup>/dRyr<sup>GS21220</sup>*.

To increase *dRyr* gene copy number, we inserted an additional genomic copy of *dRyr* into chromosome 3 to generate the *dRyr* duplication strain, *dRyr<sup>24D03</sup>* (fig. 1A). *dRyr<sup>24D03</sup>* rescued the halothane-resistant phenotype of *dRyr<sup>GS21220</sup>/+*

(fig. 2B), with the shift in  $EC_{50}$  of *dRyr<sup>GS21220</sup>/+*; *dRyr<sup>24D03</sup>/+* significantly reduced from *dRyr<sup>GS21220</sup>/+* ( $P < 0.0001$ , one-way ANOVA and Bonferroni–Dunn *post hoc* tests), and not different from the wild-type. Combining *dRyr<sup>24D03</sup>* into a wild-type background, resulting in three copies of *dRyr*, caused significant hypersensitivity to halothane (*i.e.*, a shift in  $EC_{50}$  of  $-19\%$ ; fig. 2B). Additional copies of *dRyr<sup>24D03</sup>* produced lethality, suggesting that no more than three copies of the gene can be tolerated. Importantly, the mutants' altered response to halothane did not result from nonspecific hyperactivity or arousal, in that all performed normally or worse than wild-type animals when tested for locomotion and responsiveness to mechanical stimulation in the absence of anesthetic (fig. 2C).

As was the case for the *dRyr* insertion mutants (fig. 1C), there was a significant effect of *dRyr* genotype on dRyr protein levels (fig. 2D;  $P < 0.0001$ , one-way ANOVA). In Bonferroni–Dunn *post hoc* tests, dRyr protein was

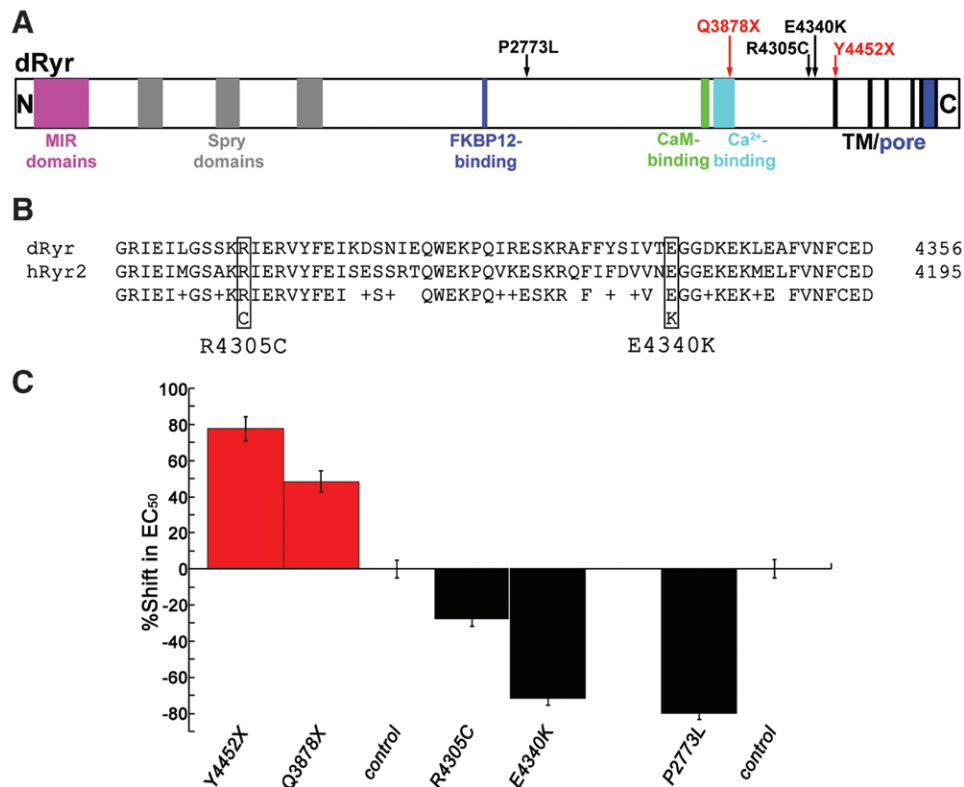


**Fig. 3.** Point mutations in *dRyr* change halothane sensitivity of *Drosophila*. (A) Schematic illustration shows predicted motifs in the primary sequence of *Drosophila* Ryr, including MIR domains, SPRY domains, FKBP12-binding domain, Ca<sup>2+</sup>-binding domain, calmodulin-binding domain, six transmembrane segments (TM), and the Ca<sup>2+</sup> pore. Sites of amino acid alterations (arrows) in the five *dRyr* alleles described in the main text. Red arrows indicate nonsense mutations and black arrows indicate missense mutations. (B) Alignment of *dRyr* (top line, accession NP\_476994.1) and the human cardiac Ryr, hRyr2 (second line, accession NP\_001026.2), in the region spanning the missense alleles *dRyr<sup>R4305C</sup>* and *dRyr<sup>E4340K</sup>*. Sites of amino acid substitutions are indicated by boxes. In the third line, identities between the sequences are indicated by the amino acid symbol, conservative substitutions are indicated by plus signs, and nonconservative substitutions are indicated by blank spaces. (C) Point mutations in *dRyr* alter halothane sensitivity. Nonsense mutations *dRyr<sup>Y4452X</sup>/+* and *dRyr<sup>Q3878X</sup>/+* (red) are resistant to halothane, whereas missense mutations *dRyr<sup>R4305C</sup>/+*, *dRyr<sup>E4340K</sup>/+*, and *dRyr<sup>P2773L</sup>/+* (black) display hypersensitivity to halothane. All mutant values are significantly different from their matched wild-type controls ( $P = 0.0043$  for *dRyr<sup>R4305C</sup>/+* and  $P < 0.0001$  for all others, one-way ANOVA and Bonferroni–Dunn *post hoc* tests). Values are mean  $\pm$  SEM. *dRyr* = *Drosophila* Ryr.



strongly and significantly reduced in  $dRyr^{\Delta 25}/+$  and  $dRyr^{\Delta 25}/dRyr^{GS21220}$ . The increase in dRyr protein in  $dRyr^{24D03}/+$  did not reach significance.

Taken together, our results demonstrate that halothane sensitivity follows  $dRyr$  gene copy number and protein levels. We conclude that dRyr is a limiting factor for halothane-induced anesthesia and a likely target of halothane.

### ***dRyr Point Mutations Change Halothane Sensitivity***

Although copy number variation in humans is well-documented, most disease-associated mutations in human *Ryr* (*hRyr*) genes are amino acid substitutions that lead to dominant alleles.<sup>11,29</sup> dRyr is 45–47% identical in primary sequence to the three mammalian Ryrs and contains conserved protein domains important to Ryr function (fig. 3A), indicating that Ryr activity and regulation may be conserved across species.

Previous work had identified a collection of lethal EMS mutants in region 44D–45F.<sup>30,31</sup> Using NextGen sequencing, we determined that five of these mutants [ $l(2)44Fa^3$ ,  $l(2)44Fg^1$ ,  $l(2)44Fh^1$ ,  $l(2)44Fj^1$ , and  $l(2)44Fp^1$ ] altered the sequence of  $dRyr$  (table 1; fig. 3, A and B). Two of these  $dRyr$  alleles contained nonsense mutations at positions corresponding to amino acid 3878 (Q3878X) in  $l(2)44Fa^3$ , and at 4452 (Y4452X) in  $l(2)44Fj^1$ . In both alleles, mutations introduced a stop codon before the transmembrane region containing the ion channel, producing truncated and nonfunctional dRyrs. As expected for loss-of-function alleles, heterozygotes were resistant to halothane ( $dRyr^{Y4452X}/+$ , 78% shift,  $dRyr^{Q3878X}/+$ , 48% shift compared to genetically matched control strain  $l(2)44Ff^1$ ; fig. 3C;  $P < 0.0001$  and  $P < 0.0001$ , one-way ANOVA and Bonferroni–Dunn *post hoc* tests) and both failed to complement the lethal phenotype of  $dRyr^{\Delta 25}$ . The relative magnitude of halothane resistance in the point mutants appeared to be larger than that of the deletion allele  $dRyr^{\Delta 25}$  (fig. 2A), but differences in genetic backgrounds of the animals in the two experiments make comparisons problematic.

The three other alleles were missense mutations, leading to substitutions of highly conserved amino acids: R4305C in  $l(2)44Fg^1$ , E4340K in  $l(2)44Fh^1$ , and P2773L in  $l(2)44Fp^1$  (table 1; fig. 3, A and B). All of the missense mutations were lethal in combination with  $dRyr^{\Delta 25}$ , two of the mutations are located in a region associated with dominant

channelopathies in hRyr2 (see below under Ryr and Neuropathology for details), and all exhibited dominant hypersensitivity to halothane (fig. 3C). Halothane sensitivity was enhanced in  $dRyr^{R4305C}/+$  (–28% shift in  $EC_{50}$ ,  $P = 0.0043$ , one-way ANOVA and Bonferroni–Dunn *post hoc* tests), and strongly increased in  $dRyr^{E4340K}/+$  and  $dRyr^{P2773L}/+$  (–72% and –80%, respectively;  $P < 0.0001$ , one-way ANOVA and Bonferroni–Dunn *post hoc* tests; fig. 3C). Thus, the missense mutations in  $dRyr$  produced dominant effects on halothane anesthesia in *Drosophila*, resembling the gain-of-function phenotype caused by an extra copy of  $dRyr$  (fig. 2B).

### ***dRyr Function in the Nervous System Is Required for Normal Halothane Sensitivity***

In the human disease malignant hyperthermia, mutations in *hRyr1* are associated with a potentially fatal condition in which skeletal muscle Ryrs activate in response to volatile anesthetics, particularly halothane. Because the reactive climbing assay is based on locomotion, and could therefore be influenced by dRyr action in muscle, we determined the site of action of dRyr by driving the expression of double-stranded RNA ( $UAS-dRyr^{RNAi}$ ) using tissue-specific *GAL4* drivers. Importantly, driving  $UAS-dRyr^{RNAi}$  with the muscle-specific driver *MHC-GAL4* failed to alter halothane sensitivity compared to controls carrying *MHC-GAL4* alone (fig. 4A;  $P = 1$ , two-way ANOVA and Bonferroni–Dunn *post hoc* tests). By contrast, flies expressing  $UAS-dRyr^{RNAi}$  under the control of the pan-neuronal drivers *elav-GAL4* and *Appl-GAL4* were significantly resistant to halothane (36% and 25% shift in  $EC_{50}$ , respectively; fig. 4A;  $P < 0.0001$  and  $P = 0.0094$ ), suggesting that dRyr function is required in neurons for normal halothane sensitivity. Interestingly, driving  $UAS-dRyr^{RNAi}$  expression in glia with *repo-GAL4* also produced significant resistance to halothane (22% shift in  $EC_{50}$ ;  $P = 0.0373$ ), indicating that dRyr is required in glia and neurons for halothane anesthesia. When driven by *nrv2-GAL4*, which expresses broadly but not ubiquitously in neurons and glia,  $UAS-dRyr^{RNAi}$  produced a small (16%) but not statistically significant shift in  $EC_{50}$  (fig. 4A;  $P = 0.0862$ ).

To further establish the site of action of dRyr, we sought to restore halothane sensitivity in dRyr mutants by expressing a  $UAS-dRyr$  transgene in selected cell types. Although expression of the rescue construct using the exclusively

**Table 1.** Point Mutations Identified in dRyr\*

Mutant†	Mutation in dRyr mRNA‡	Amino Acid Change§	Halothane Phenotype
$l(2)44Fa^3$	C11786T	Q3878X	Resistance
$l(2)44Fj^1$	T13510A	Y4452X	Resistance
$l(2)44Fg^1$	C13067T	R4305C	Resistance
$l(2)44Fh^1$	G13172A	E4340K	Hypersensitivity
$l(2)44Fp^1$	C8472T	P2773L	Hypersensitivity

\* dRyr, *Drosophila* ryanodine receptor. †  $l(2)44F$ , lethal mutation on chromosome 2, cytologic position 44F. ‡  $dRyr$  transcript variant D (NM\_057646.2). § dRyr isoform D (NP\_476994.1).



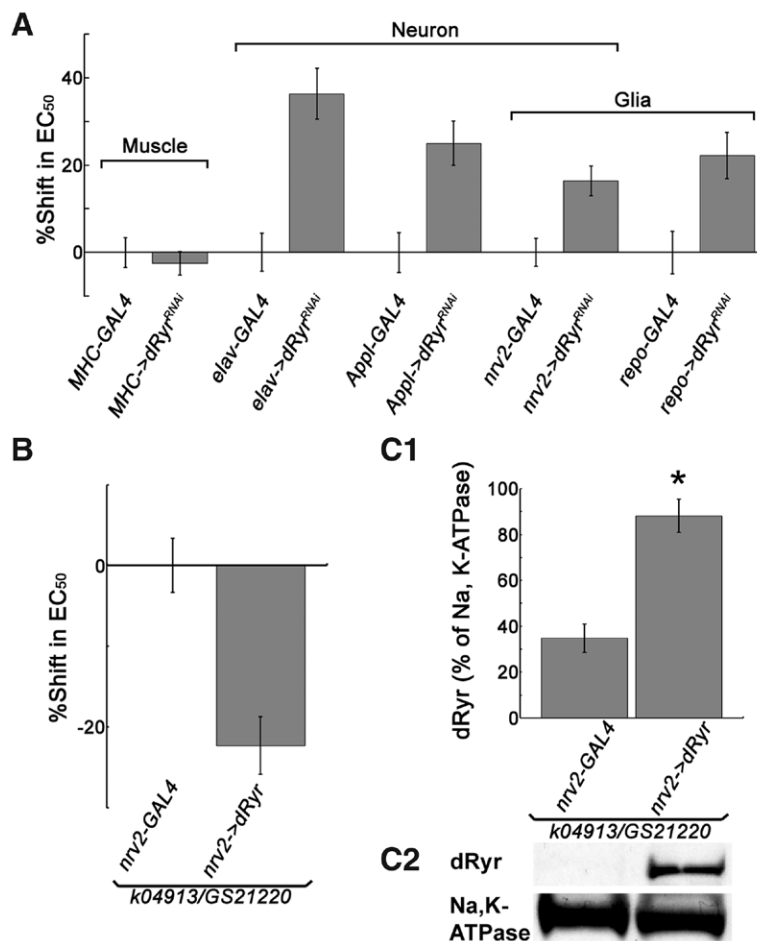


**Fig. 4.** dRyr expressed in the nervous system is required for normal halothane sensitivity. (A) dRyr activity in the nervous system, but not in muscle, is required for normal halothane sensitivity in *Drosophila*. Flies expressing RNAi against *dRyr* (*UAS-dRyr<sup>RNAi</sup>*) under the control of the muscle-specific driver *MHC-GAL4* (*MHC->dRyr<sup>RNAi</sup>*) are not different from controls (*MHC-GAL4* alone) in the reactive climbing assay for halothane ( $P = 1$ , two-way ANOVA and Bonferroni-Dunn *post hoc* tests). In contrast, *elav->dRyr<sup>RNAi</sup>* and *Appl->dRyr<sup>RNAi</sup>* flies, in which dRyr expression in neurons is specifically inhibited, display strong resistance to halothane compared to controls (*elav-GAL4* and *Appl-GAL4*, respectively). Expressing *UAS-dRyr<sup>RNAi</sup>* using the glia-specific driver *repo-GAL4* (*repo->dRyr<sup>RNAi</sup>*) significantly increases resistance to halothane ( $P = 0.0373$ , two-way ANOVA and Bonferroni-Dunn *post hoc* tests). Broad expression in neurons and glia, driven by *nrv2-GAL4* (*nrv2->dRyr<sup>RNAi</sup>*), does not cause significant resistance ( $P = 0.0862$ , two-way ANOVA and Bonferroni-Dunn *post hoc* tests). Values are mean  $\pm$  SEM. (B) dRyr expressed in the nervous system is sufficient for halothane sensitivity. Restoring dRyr expression in the nervous system using *nrv2-GAL4* to drive *UAS-dRyr* rescues the resistant phenotype in mutant *dRyr<sup>k04913</sup>/dRyr<sup>GS21220</sup>*. (C) Restoring dRyr expression in the nervous system in rescue flies (*dRyr<sup>k04913</sup>/dRyr<sup>GS21220</sup>*, *nrv2->dRyr*) is confirmed by Western blot of membrane extracts from fly heads. (C1) The bar graph shows that dRyr levels increase significantly (asterisk) over the negative control ( $P < 0.0001$ , Student *t* test;  $n = 8$ ). Values are mean  $\pm$  SEM. (C2) Representative Western blot. As shown in the bar graph, dRyr protein is present in the mutants but is not visible in this exposure. *dRyr* = *Drosophila Ryr*.

muscle-, neuron-, and glia-specific drivers proved lethal, expression in neurons and glia using *nrv2-GAL4* restored sensitivity to halothane in transheterozygous *dRyr<sup>k04913</sup>/dRyr<sup>GS21220</sup>* mutants ( $-22\%$  shift in EC<sub>50</sub>; fig. 4B;  $P < 0.0001$ , Student *t* test). This manipulation also restored dRyr protein expression in the brains of rescued flies, as shown by Western blots of head extracts (fig. 4C;  $P < 0.0001$ , Student *t* test).

In summary, tissue-specific knockdown and rescue experiments support the conclusion that dRyr functions in the nervous system and not muscle to control anesthetic responsiveness of *Drosophila*. In addition, the lethality resulting

from *UAS-dRyr* overexpression in most tissues, combined with the observation that homozygous *dRyr<sup>24D03</sup>* and *dRyr<sup>A25</sup>* are lethal, indicates that temporal or spatial variation in dRyr expression levels are poorly tolerated, presumably because of its critical role in cellular calcium homeostasis.

#### Halothane Induces Ca<sup>2+</sup> Release in dRyr-transfected Sf9 Cells

The results described in the previous section demonstrate that dRyr in the nervous system is required for full susceptibility to halothane, but the ability of halothane to

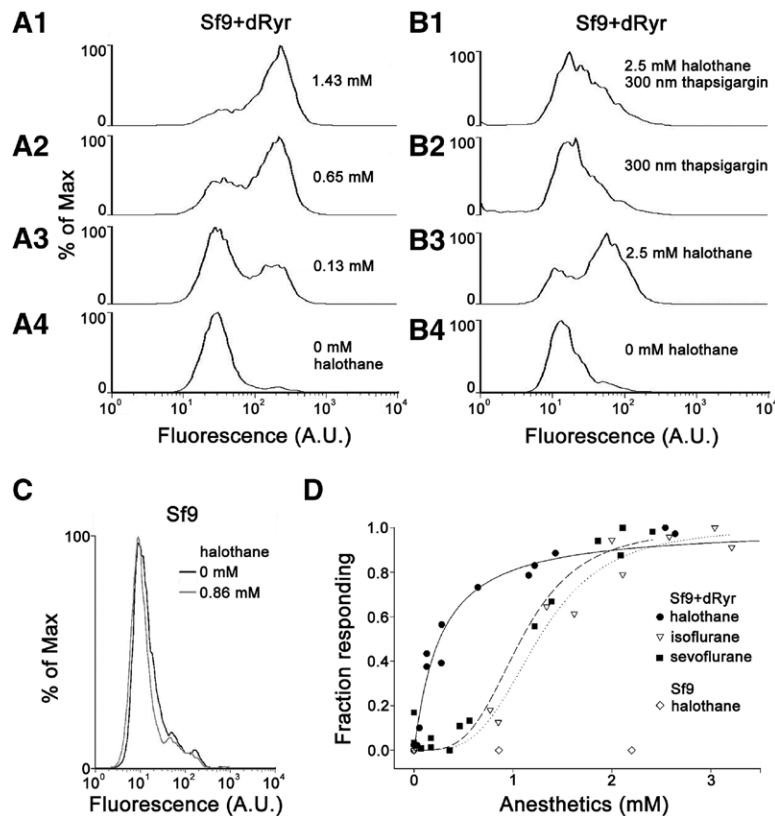


**Fig. 5.** Halothane induces  $\text{Ca}^{2+}$  release from internal stores in Sf9 cells stably transfected with *dRyr* (Sf9+dRyr). Flow cytometry was used to measure  $[\text{Ca}^{2+}]_i$  in Sf9 cells loaded with Fluo-5 AM. (A) Representative histograms from flow cytometric analysis of Sf9+dRyr cells treated with halothane. Plots show the number of cells at each level of fluorescence (A.U. = arbitrary units), normalized to the modal value (% of Max). (A1) Treatment with 1.43 mM halothane results in a high proportion of cells with high fluorescence intensity. (A2 and A3) Intermediate concentrations of halothane shift the proportions of cells with high versus low fluorescence. (A4) In the absence of halothane, Sf9+dRyr cells show low levels of fluorescence. Each histogram represents 10,000 cells. (B) Depletion of intracellular  $\text{Ca}^{2+}$  with thapsigargin blocks the halothane-induced  $[\text{Ca}^{2+}]_i$  increase in Sf9+dRyr cells. (B1) Pretreatment with thapsigargin, which blocks the sarcoplasmic/endoplasmic reticulum  $\text{Ca}^{2+}$  ATPase and results in store depletion, blocks the effect of halothane, compared to cells treated with thapsigargin alone (B2). (B3) Treatment of cells with a high concentration of halothane (2.5 mM); the majority show elevated fluorescence compared with untreated cells (B4). Note that a subpopulation of cells in this experiment did not respond to halothane. (C) Untransfected Sf9 cells do not respond to halothane. Fluorescence does not increase in Sf9 cells treated with 0.86 mM halothane (gray line) compared with untreated controls (black line). (D) Concentration–response curves for anesthetic-induced  $\text{Ca}^{2+}$  flux. Each data point represents the proportion of cells with elevated  $[\text{Ca}^{2+}]_i$  in a sample of 10,000 cells. The proportion of Sf9+dRyr cells with elevated  $[\text{Ca}^{2+}]_i$  increases as a function of anesthetic concentration, with halothane (filled circles) being manyfold more potent than sevoflurane (filled squares) or isoflurane (open triangles) in stimulating  $\text{Ca}^{2+}$  release via dRyr. Untransfected Sf9 cells do not respond to halothane (open diamonds), even at high concentrations (>2 mM). *dRyr* = *Drosophila Ryr*.

activate the *Drosophila* Ryr has not been tested. We therefore assayed  $\text{Ca}^{2+}$  flux in Sf9 cells stably transfected with *dRyr* (Sf9+dRyr),<sup>20</sup> using the  $\text{Ca}^{2+}$ -sensitive dye Fluo-5 and flow cytometry (fig. 5). Without halothane, the intensity of Fluo-5 fluorescence in Sf9+dRyr cells (fig. 5, A4) corresponded to  $[\text{Ca}^{2+}]_i$  between 50 and 100 nM. Treatment with halothane concentrations greater than 1 mM shifted fluorescence to a much higher level in almost all transfected cells (fig. 5, A1), with calibrated  $[\text{Ca}^{2+}]_i$  exceeding 100  $\mu\text{M}$ . Pretreatment of transfected cells with 300 nM thapsigargin to deplete intracellular calcium stores blocked the halothane-induced  $[\text{Ca}^{2+}]_i$  increase (fig. 5B), confirming that the response to halothane depends on internal  $\text{Ca}^{2+}$  stores. Halothane had no effect on

untransfected Sf9 cells (fig. 5C), even at high concentrations (fig. 5D, open diamonds), indicating that the response to halothane required dRyr.

Curiously, individual Sf9+dRyr cells responded to halothane in an all-or-none manner, exhibiting either basal or maximal levels of  $[\text{Ca}^{2+}]_i$  at any given halothane concentration (fig. 5, A2 and A3). Concentration–response curves were thus analyzed as the proportion of cells producing elevated  $[\text{Ca}^{2+}]_i$  in response to drug application. Analyzed in this way, the  $\text{EC}_{50}$  for caffeine ( $1.42 \pm 0.96$  mM), for which the response is completely dependent on dRyr expression, was similar to the previously published value.<sup>20</sup> For anesthetics, concentration–response relationships

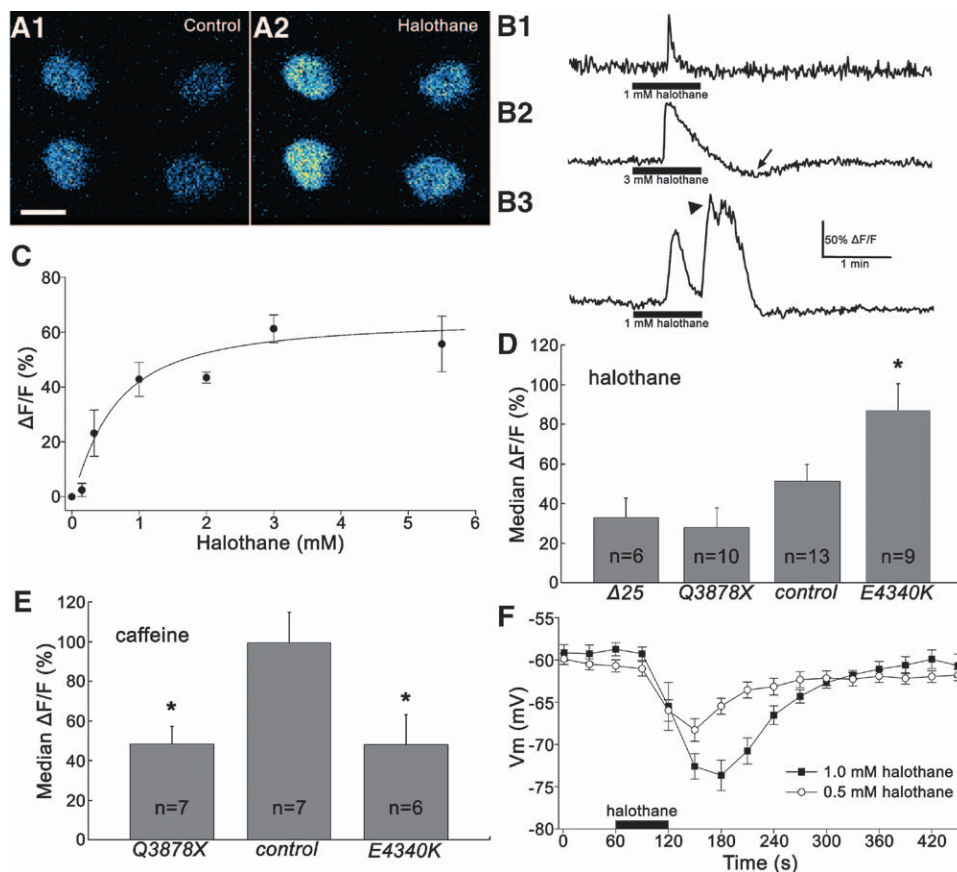


**Fig. 6.** Halothane increases  $[Ca^{2+}]_i$  and hyperpolarizes motoneuron RP2. (A) Halothane treatment increases  $[Ca^{2+}]_i$  in larval motoneuron RP2. Changes in  $[Ca^{2+}]_i$  in RP2 cell bodies are visualized using the genetically encoded  $Ca^{2+}$  indicator *UAS-GCaMP3* driven by *ShakB-GAL4*. As shown in this false color image of four cells in two abdominal segments,  $[Ca^{2+}]_i$  increases with the addition of halothane (2.5 mM). Scale bar = 10  $\mu$ m. (B) Representative traces of calcium transients observed in the somata of RP2 neurons with halothane treatment. The entire soma was defined as the region of interest, and fluorescence intensity was converted into a percentage change ( $\Delta F/F$ ) as described earlier under Experimental Procedures. (B1) All cells produced an immediate response, with a sharp rise that occurred within a short period of halothane entering the chamber.  $[Ca^{2+}]_i$  began to decay before halothane was removed. (B2) At higher concentrations, a pronounced undershoot, in which  $[Ca^{2+}]_i$  dropped below baseline, followed halothane removal (arrow). (B3) A minority of cells produced a delayed response at the time of halothane removal, consisting of a plateau with superimposed spiky transients (arrowhead). (C) The concentration–response relationship for the peak amplitude of the halothane-induced calcium transient response in RP2 neurons. RP2 responded to halothane in a concentration-dependent manner, with  $EC_{50} = 0.61$  mM. Values are mean  $\pm$  SEM ( $n = 3$ –8 preparations per data point). (D) *dRyr* mutations affect RP2's response to halothane. RP2 neurons in larvae heterozygous for *dRyr*<sup>E4340K</sup>, which causes hypersensitivity to halothane in adult flies, respond more strongly to 0.5 mM halothane than controls. In contrast, halothane appears to induce smaller responses in RP2 neurons heterozygous for the deletion mutant *dRyr* <sup>$\Delta 25$</sup>  and the nonsense mutation *dRyr*<sup>Q3878X</sup>. Error bars represent SEM, and asterisk denotes statistical significance by one-way ANOVA and Bonferroni–Dunn *post hoc* tests ( $P = 0.0484$ ). (E) *dRyr* mutations reduce sensitivity to caffeine. RP2 motoneurons from larvae heterozygous for *dRyr*<sup>Q3878X</sup> and *dRyr*<sup>E4340K</sup> respond more weakly to 5 mM caffeine than controls ( $P = 0.0375$  and  $P = 0.0453$ , one-way ANOVA and Bonferroni–Dunn *post hoc* tests). (F) Halothane hyperpolarizes wild-type RP2 neurons. In whole-cell current clamp recordings, halothane application produces a strong hyperpolarization that is proportional to halothane concentration. Recovery is delayed at 1 mM compared to 0.5 mM halothane. Membrane potentials are recorded using whole-cell current clamp recording. Values are mean  $\pm$  SEM ( $n = 5$ –7). *dRyr* = *Drosophila Ryr*.

showed strong selectivity for halothane (fig. 5D), with  $EC_{50}$  values of 0.26, 1.1, and 1.3 mM for halothane, sevoflurane, and isoflurane, respectively. Converted to partial pressures, these values correspond to 0.48%, 1.9%, and 2.6% atm, indicating that halothane is manyfold more potent than either sevoflurane or isoflurane. We propose that molecular interactions between halothane and the *dRyr* protein

explain the selective sensitivity of *dRyr* mutants to halothane anesthesia in *Drosophila* (fig. 1D).

#### Halothane Increases $[Ca^{2+}]_i$ and Hyperpolarizes Motoneuron RP2

To examine the effects of halothane on  $Ca^{2+}$  flux in central neurons of *Drosophila*, we drove the expression of the

genetically encoded  $\text{Ca}^{2+}$  indicator GCaMP3<sup>22</sup> in larval motoneuron RP2 using *ShakB-GAL4*. RP2 responded to halothane with robust increases in GCaMP3 fluorescence, clearly visible in unprocessed images (fig. 6A).

All cells produced an immediate response to halothane application that peaked during the short period of halothane entering the chamber (fig. 6B). The amplitude of this immediate response showed a robust concentration–response relationship (fig. 6C), with an  $\text{EC}_{50}$  for halothane of 0.61 mM. A pronounced undershoot, during which  $[\text{Ca}^{2+}]_i$  fell below resting levels, was routinely observed, particularly in response to high concentrations of halothane (fig. 6, B2). A minority of cells produced an additional delayed response, consisting of a plateau overlaid with spiky transients, at or near the time of halothane removal (fig. 6, B3).

The response of RP2 to halothane was altered by mutations in *dRyr* (fig. 6D). In preparations heterozygous for the deletion mutant, *dRyr*<sup>Δ25</sup>, and the presumed truncation, *dRyr*<sup>Q3878X</sup>, the GCaMP3 responses to 0.5 mM halothane were reduced by more than 30% and more than 50%, respectively. Although consistent with a reduced response, these differences did not reach statistical significance ( $P = 1$  and  $P = 0.6008$ , one-way ANOVA and Bonferroni–Dunn *post hoc* tests). However, RP2 motoneurons heterozygous for point mutant *dRyr*<sup>E4340K</sup>, which causes dominant hypersensitivity in the reactive climbing assay (fig. 3C), responded to halothane with significantly larger  $\text{Ca}^{2+}$  flux (fig. 6D;  $P = 0.0484$ ), indicating that this allele enhances the response of dRyr to halothane. The hypersensitivity of *dRyr*<sup>E4340K</sup> for both reactive climbing and  $\text{Ca}^{2+}$  release suggests that it is a gain-of-function allele for halothane action.

The response of RP2 motoneurons to caffeine provided additional insight into the nature of the mutations. Wild-type RP2 neurons' responses to caffeine were similar to those of other insect neurons,<sup>20</sup> with an  $\text{EC}_{50}$  of  $5.4 \pm 2.4$  mM. When challenged with 5 mM caffeine, the change in fluorescence in *dRyr*<sup>Q3878X/+</sup> was significantly lower than in the wild-type (fig. 6E;  $P = 0.0375$ , one-way ANOVA and Bonferroni–Dunn *post hoc* tests). Surprisingly, the caffeine response of neurons heterozygous for *dRyr*<sup>E4340K</sup> was also smaller than normal (fig. 6E;  $P = 0.0453$ ), to an extent similar to that of *dRyr*<sup>Q3878X</sup>. Therefore, the E-to-K substitution enhances the response to halothane but reduces the response to caffeine, indicating that the mutation selectively alters the response of dRyr depending on the nature of the signal. This conditional loss-of-function phenotype may also explain the lethality of *dRyr*<sup>E4340K/dRyr</sup><sup>Δ25</sup>, in that the substitution may disable dRyr for a vital function.

In whole-cell, current clamp recordings of RP2, halothane evoked a strong, concentration-dependent hyperpolarization (fig. 6F). Importantly, there was no evidence of depolarization or spiking that would indicate  $\text{Ca}^{2+}$  flux through channels in the plasma membrane. Instead, the

membrane hyperpolarized 10–15 mV, depending on the halothane concentration. Onset and recovery both required approximately 2 min, although recovery was delayed at the higher concentration. Therefore, the  $\text{Ca}^{2+}$  flux demonstrated by imaging with GCaMP3 is paralleled by a robust hyperpolarization of the motoneuron, suggesting the activation of an inhibitory conductance.

## Discussion

The molecular and cellular mechanisms of volatile anesthetic action have been the subject of intensive study for decades. This interest derives not only from the great medical importance of anesthesia but also from the conviction that understanding the molecular and neural pathways that mediate anesthetic effects will provide insight into the nature of arousal and consciousness. Additional interest has been generated recently by the finding that general anesthesia contributes to various neuropathologic conditions. Despite these convergent interests, the search for biologically relevant protein targets of volatile anesthetics has produced few confirmed candidates. The present study demonstrates that in *Drosophila* the ryanodine receptor (dRyr) is likely to represent such an anesthetic target. We show that neurally expressed dRyr mediates the behavioral response to the volatile anesthetic halothane, with whole-animal sensitivity to halothane anesthesia strongly dependent on gene dosage of *dRyr*. Point mutations in the *dRyr* gene that generate truncated, and therefore nonfunctional, proteins cause resistance to halothane, whereas missense mutations that alter highly conserved amino acids make flies more sensitive to the anesthetic. Our demonstration that the dRyr imparts halothane sensitivity to Sf9 cells, and that neurons in central nervous systems isolated from halothane-sensitive *dRyr* mutants exhibit elevated  $\text{Ca}^{2+}$  influx specifically in response to halothane, further support the conclusion that dRyr is a *bona fide* target of the anesthetic.

### *dRyr* in the Nervous System Mediates Halothane Sensitivity

The data presented here show that the potency of halothane is proportional to *dRyr* function. Reduction of function, as described for heterozygous *dRyr*<sup>K04913</sup>, *dRyr*<sup>GS21220</sup>, *dRyr*<sup>Δ25</sup>, or their heteroallelic combinations, causes resistance to halothane. Moreover, point mutants that are predicted to produce truncated, and therefore nonfunctional dRyr channels, also produce dominant resistance. Conversely, an additional genomic copy of dRyr confers hypersensitivity to halothane.

Importantly, tissue-specific knockdown and rescue experiments demonstrated that *dRyr* function in neurons and glia, but not muscle, is necessary for normal susceptibility to halothane anesthesia and that dRyr expression in these cells is sufficient to impart anesthetic sensitivity. The Ryr-dependent anesthetic phenotypes are therefore clearly distinct from those found in malignant hyperthermia, a



condition associated with mutations that cause halothane hypersensitivity of the skeletal muscle isoform, *Ryr1*, in humans and swine. This conclusion is underscored by the finding that RNAi-mediated knockdown of dRyr expression in muscle fails to alter the halothane sensitivity of reactive climbing.

The observation that both the *Drosophila* Ryr and the mammalian muscle isoform of this receptor, Ryr1, mediate halothane-sensitive physiologic processes suggests that halothane sensitivity is a general property of Ryrs. Indeed, in cardiac myocytes and neurons, which express predominantly Ryr2 and Ryr3, respectively, halothane induces Ryr-dependent  $\text{Ca}^{2+}$  flux from intracellular stores.<sup>32–34</sup> This is consistent with our observations that dRyr mediates halothane-dependent  $\text{Ca}^{2+}$  flux in *Drosophila* motoneurons, and supports a proposal that neural Ryrs mediate the immobilizing effects of anesthetics.

### Mechanisms of Ryr Activation

Although regulation of Ryr function is complex, two principal mechanisms have been defined for its activation:  $\text{Ca}^{2+}$ -mediated activation and interaction with accessory proteins.<sup>35</sup> If halothane activates Ryr by elevating intracellular  $\text{Ca}^{2+}$  levels, it must do so either by promoting  $\text{Ca}^{2+}$  entry from the extracellular space or by causing release from intracellular stores. Flow cytometry results reported here show that elevation of internal  $\text{Ca}^{2+}$  is not observed in Sf9 cells, even at high levels of halothane, unless they have been transfected with dRyr. Moreover, it has been shown previously that halothane can activate isolated Ryr1 channels in membrane preparations.<sup>36</sup> This argues against activation of dRyr by  $\text{Ca}^{2+}$ -induced  $\text{Ca}^{2+}$  release.

Although it remains possible that halothane activates Ryr indirectly by interacting with one of its many accessory proteins, this explanation would require that Sf9 cells, which do not normally express detectable Ryr,<sup>20</sup> produce the critical, halothane-dependent accessory subunit(s) when transfected with dRyr. We instead favor the hypothesis that halothane interacts directly with the dRyr protein. The absence of the full complement of regulatory subunits in Sf9+dRyr cells may in fact explain the curious bimodal pattern of the response of Sf9+dRyr cells to halothane. If Sf9 cells do not express a protein such as sorcin, which has been postulated to help terminate  $\text{Ca}^{2+}$ -induced  $\text{Ca}^{2+}$  release,<sup>35</sup> activation of dRyr by halothane could initiate a positive feedback loop of  $\text{Ca}^{2+}$  release, in which a small increase of cytoplasmic  $\text{Ca}^{2+}$  would initiate a flood of  $\text{Ca}^{2+}$  in the cytoplasm.

In contrast to the all-or-none response of Sf9+dRyr cells, RP2 motoneurons responded to halothane with transient, concentration-dependent  $\text{Ca}^{2+}$  flux. The transient nature of the signal suggests that either dRyrs inactivate in the continued presence of halothane, or that  $\text{Ca}^{2+}$  is rapidly removed from the cytoplasm. The transient reduction of GCaMP3 fluorescence below baseline levels on removal of halothane

is consistent with robust activation of mechanisms for extrusion and sequestration of intracellular  $\text{Ca}^{2+}$ .

### Downstream Effectors

$\text{Ca}^{2+}$  released by halothane-dependent activation of dRyr must ultimately change neuronal excitability to contribute to the anesthetic state. Observations in mammals and worms show that neuronal hyperpolarization is a common feature of halothane anesthesia,<sup>4,5</sup> consistent with our electrophysiologic recordings of RP2 motoneurons. The ultimate effector of Ryr activation is thus likely to be an inhibitory conductance, possibly carried by a  $\text{K}^{+}$  channel.  $\text{Ca}^{2+}$ -activated  $\text{K}^{+}$  channels are obvious candidates, but it is interesting to speculate that the rapid and robust removal of excess  $\text{Ca}^{2+}$  from the cytoplasm may provide a novel route to  $\text{K}^{+}$  channel activation.  $\text{Ca}^{2+}$  extrusion by the plasma membrane  $\text{Ca}^{2+}$  adenosine triphosphatase, which exchanges internal  $\text{Ca}^{2+}$  for external  $\text{H}^{+}$ , can result in cytoplasmic acidification,<sup>37</sup> which could in turn activate K2P channels, such as TREK-1, which are sensitive to low internal pH.<sup>38</sup> This mechanism could also provide an additional pathway for the actions of carbon dioxide, which is membrane permeant, causes acidification through the action of carbonic anhydrase, and acts as an anesthetic.<sup>39</sup> The merits of these and competing hypotheses remain to be tested, but the work described here shows that the genetic and physiologic tools readily available in *Drosophila* should be useful in doing so.

### Ryr and Neuropathology

The intimate relationship between dRyr activity and halothane anesthesia has possible implications regarding the association between volatile anesthetics and cytotoxicity, neurodegeneration, and cognitive deficits, pathologic conditions often associated with dysregulation of intracellular  $\text{Ca}^{2+}$  levels.<sup>40</sup> It is also interesting in this regard that two of the three point mutations in *dRyr* that we found to enhance sensitivity to halothane are in a region associated with human cellular abnormality.

*dRyr*<sup>E4340K</sup> is adjacent to a mutation in *hRyr2* (*i.e.*, N4178S) that is associated with multiple cases of catecholaminergic polymorphic ventricular tachycardia, a condition characterized by exercise-induced cardiac arrhythmia.<sup>29</sup> Perhaps most interestingly, *dRyr*<sup>R4305C</sup> is a substitution identical to that causing sudden cardiac death (*hRyr2*<sup>R4144C</sup>).<sup>41</sup> All three missense mutations increase the potency of halothane in our reactive climbing assay, and one enhances the halothane-evoked release of  $\text{Ca}^{2+}$  in RP2 motoneurons, suggesting shared mechanisms of Ryr-dependent  $\text{Ca}^{2+}$  dysregulation among different isoforms and across phyla. Of particular interest is the observation that the amino acid substitution in *dRyr*<sup>E4340K</sup> enhances sensitivity to halothane but blocks activation by caffeine, indicating that the mutant protein is not simply hyperactive. Similar mutations in neurally expressed Ryr in humans may predispose individuals to the cytotoxic effects of anesthetics. In support of this hypothesis,

halothane produces altered electroencephalographic activity during episodes of malignant hyperthermia in susceptible swine.<sup>42</sup>

The emerging picture based on investigation of the mechanisms of anesthesia in genetic model organisms is that, despite the identical endpoint of immobility, each volatile anesthetic is likely to act through its own collection of molecular targets. The collection of targets mediating halothane anesthesia now includes Ryr. At present, it is unclear how completely the mechanisms uncovered in invertebrate models, such as flies and worms, will translate to mammalian anesthesia. In mammals, immobilization by volatile anesthetics is likely to be mediated by spinal circuitry.<sup>4</sup> The insect ventral nerve cord and motoneurons such as RP2 are functional analogs of the mammalian spinal cord and spinal motoneurons, respectively. However, the degree of homology between the segmental neuromeres of insects and mammals is not fully understood, and therefore the level of conservation of molecular targets of anesthetics remains to be established.

Remaining open questions regard the identities of the cells required to mediate immobility and the precise cellular sites of action. Our knockdown and rescue experiments manipulated dRyr expression in large numbers of neurons and glia, and it will be necessary to drive dRyr expression in subsets of these cells to determine whether anesthesia depends on the activity of a few cells or a large population. Furthermore, although halothane elicits Ca<sup>2+</sup> flux in neuronal cell bodies that correlates with hyperpolarization, we have established neither the causal link between Ca<sup>2+</sup> flux and membrane potential, nor the most important subcellular location (*e.g.*, axon, dendrite, synapse) of dRyr function. These questions provide fertile territory for subsequent investigations.

The authors thank David Ide, B.A. (Research Assistant, Research Services Branch, National Institute of Mental Health, National Institutes of Health, Bethesda, Maryland), and the Research Services Branch for construction of equipment; Daniel Cordova, M.Sc. (Senior Biochemist, Dupont Crop Protection, Newark, Delaware), for the anti-dRyr antibody, Sf9+dRyr cells, and Ryr-V5 plasmid; Ted Usdin, Ph.D., M.D. (Senior Investigator, National Institute of Mental Health, National Institutes of Health, Bethesda, Maryland), for the use of culture facilities; Robert L. Scott, M.Sc. (Research Assistant, National Institute of Mental Health, National Institutes of Health, Bethesda, Maryland), for technical assistance and comments on the article; Songling Huang, Ph.D. (Senior Data Analyst, TurningPoint Global Solutions, Rockville, Maryland) and Gang Chen, Ph.D. (Mathematical Statistician, National Institute of Mental Health, National Institutes of Health, Bethesda, Maryland), for statistical consultation; Qun Gu, A.A. (Research Assistant, National Institute of Mental Health, National Institutes of Health, Bethesda, Maryland), for plasmid construction; Benjamin White, Ph.D. (Senior Investigator, National Institute of Mental Health, National Institutes of Health, Bethesda, Maryland), for use of equipment and help in assembling the article; and Philip Morgan, M.D. (Professor, Seattle Children's Hospital, Seattle, Washington), and Joseph Campbell, Ph.D. (Program Officer, National Institute of Allergy and Infectious Diseases, National Institutes of Health, Bethesda, Maryland), for helpful comments.

## References

1. Rudolph U, Antkowiak B: Molecular and neuronal substrates for general anaesthetics. *Nat Rev Neurosci* 2004; 5:709–20
2. Heurteaux C, Guy N, Laigle C, Blondeau N, Duprat F, Mazzuca M, Lang-Lazdunski L, Widmann C, Zanzouri M, Romey G, Lazdunski M: TREK-1, a K<sup>+</sup> channel involved in neuroprotection and general anesthesia. *EMBO J* 2004; 23:2684–95
3. Humphrey JA, Hamming KS, Thacker CM, Scott RL, Sedensky MM, Snutch TP, Morgan PG, Nash HA: A putative cation channel and its novel regulator: Cross-species conservation of effects on general anesthesia. *Curr Biol* 2007; 17:624–9
4. Lazarenko RM, Willcox SC, Shu S, Berg AP, Jevtovic-Todorovic V, Talley EM, Chen X, Bayliss DA: Motoneuronal TASK channels contribute to immobilizing effects of inhalational general anesthetics. *J Neurosci* 2010; 30:7691–704
5. Singaram VK, Somerlot BH, Falk SA, Falk MJ, Sedensky MM, Morgan PG: Optical reversal of halothane-induced immobility in *C. elegans*. *Curr Biol* 2011; 21:2070–6
6. Metz LB, Dasgupta N, Liu C, Hunt SJ, Crowder CM: An evolutionarily conserved presynaptic protein is required for isoflurane sensitivity in *Caenorhabditis elegans*. *ANESTHESIOLOGY* 2007; 107:971–82
7. Ying SW, Werner DF, Homanics GE, Harrison NL, Goldstein PA: Isoflurane modulates excitability in the mouse thalamus via GABA-dependent and GABA-independent mechanisms. *Neuropharmacology* 2009; 56:438–47
8. Campbell JL, Gu Q, Guo D, Nash HA: Genetic effects in *Drosophila* on the potency of diverse general anesthetics: A distinctive pattern of altered sensitivity. *J Neurogenet* 2009; 23:412–21
9. Connelly TJ, Coronado R: Activation of the Ca<sup>2+</sup> release channel of cardiac sarcoplasmic reticulum by volatile anesthetics. *ANESTHESIOLOGY* 1994; 81:459–69
10. Akata T, Nakashima M, Izumi K: Comparison of volatile anesthetic actions on intracellular calcium stores of vascular smooth muscle: Investigation in isolated systemic resistance arteries. *ANESTHESIOLOGY* 2001; 94:840–50
11. Treves S, Anderson AA, Ducreux S, Divet A, Bleunven C, Grasso C, Paesante S, Zorzato F: Ryanodine receptor 1 mutations, dysregulation of calcium homeostasis and neuromuscular disorders. *Neuromuscul Disord* 2005; 15:577–87
12. Sullivan KM, Scott K, Zuker CS, Rubin GM: The ryanodine receptor is essential for larval development in *Drosophila melanogaster*. *Proc Natl Acad Sci USA* 2000; 97:5942–7
13. Parks AL, Cook KR, Belvin M, Dompe NA, Fawcett R, Huppert K, Tan LR, Winter CG, Bogart KP, Deal JE, Deal-Herr ME, Grant D, Marcinko M, Miyazaki WY, Robertson S, Shaw KJ, Tabios M, Vysotskaia V, Zhao L, Andrade RS, Edgar KA, Howie E, Killpack K, Milash B, Norton A, Thao D, Whittaker K, Winner MA, Friedman L, Margolis J, Singer MA, Kopczynski C, Curtis D, Kaufman TC, Plowman GD, Duyk G, Francis-Lang HL: Systematic generation of high-resolution deletion coverage of the *Drosophila melanogaster* genome. *Nat Genet* 2004; 36:288–92
14. Venken KJ, Carlson JW, Schulze KL, Pan H, He Y, Spokony R, Wan KH, Koriabine M, de Jong PJ, White KP, Bellen HJ, Hoskins RA: Versatile [lacman] BAC libraries for transgenesis studies in *Drosophila melanogaster*. *Nat Methods* 2009; 6:431–4
15. Homer N, Merriman B, Nelson SF: BFAST: An alignment tool for large scale genome resequencing. *PLoS One* 2009; 4:e7767
16. Li H, Handsaker B, Wysoker A, Fennell T, Ruan J, Homer N, Marth G, Abecasis G, Durbin R; 1000 Genome Project Data Processing Subgroup: The Sequence Alignment/Map format and SAMtools. *Bioinformatics* 2009; 25:2078–9
17. Wang K, Li M, Hakonarson H: ANNOVAR: Functional annotation of genetic variants from high-throughput sequencing data. *Nucleic Acids Res* 2010; 38:e164
18. Alone DP, Rodriguez JC, Noland CL, Nash HA: Impact of gene copy number variation on anesthesia in *Drosophila melanogaster*. *ANESTHESIOLOGY* 2009; 111:15–24

19. Benzer S: Behavioral mutants of *Drosophila* isolated by countercurrent distribution. *Proc Natl Acad Sci USA* 1967; 58:1112-9
20. Cordova D, Benner EA, Sacher MD, Rauh JJ, Sopa JS, Lahm GP, Selby TP, Stevenson TM, Flexner L, Gutteridge S, Rhoades DF, Wu L, Smith RM, Tao Y: Anthranilic diamides: A new class of insecticides with a novel mode of action, ryanodine receptor activation. *Pest Biochem Physiol* 2006; 84:196-214
21. Tsien RY, Pozzan T, Rink TJ: T-cell mitogens cause early changes in cytoplasmic free  $Ca^{2+}$  and membrane potential in lymphocytes. *Nature* 1982; 295:68-71
22. Tian L, Hires SA, Mao T, Huber D, Chiappe ME, Chalasani SH, Petreanu L, Akerboom J, McKinney SA, Schreiter ER, Bargmann CI, Jayaraman V, Svoboda K, Looger LL: Imaging neural activity in worms, flies and mice with improved GCaMP calcium indicators. *Nat Methods* 2009; 6:875-81
23. Feng Y, Ueda A, Wu CF: A modified minimal hemolymph-like solution, HL3.1, for physiological recordings at the neuromuscular junctions of normal and mutant *Drosophila* larvae. *J Neurogenet* 2004; 18:377-402
24. Sandstrom DJ: Isoflurane reduces excitability of *Drosophila* larval motoneurons by activating a hyperpolarizing leak conductance. *ANESTHESIOLOGY* 2008; 108:434-46
25. Sandstrom DJ: Isoflurane depresses glutamate release by reducing neuronal excitability at the *Drosophila* neuromuscular junction. *J Physiol (Lond)* 2004; 558(Pt 2):489-502
26. Waud DR: On biological assays involving quantal responses. *J Pharmacol Exp Ther* 1972; 183:577-607
27. Motulsky H, Christopoulos A: *Fitting Models to Biological Data Using Linear and Nonlinear Regression: A Practical Guide to Curve Fitting*. New York, Oxford University Press, 2004
28. Hasan G, Rosbash M: *Drosophila* homologs of two mammalian intracellular  $Ca^{2+}$ -release channels: Identification and expression patterns of the inositol 1,4,5-triphosphate and the ryanodine receptor genes. *Development* 1992; 116:967-75
29. Medeiros-Domingo A, Bhuiyan ZA, Tester DJ, Hofman N, Bikker H, van Tintelen JP, Mannens MM, Wilde AA, Ackerman MJ: The RYR2-encoded ryanodine receptor/calcium release channel in patients diagnosed previously with either catecholaminergic polymorphic ventricular tachycardia or genotype negative, exercise-induced long QT syndrome: A comprehensive open reading frame mutational analysis. *J Am Coll Cardiol* 2009; 54:2065-74
30. Dockendorff TC, Robertson SE, Faulkner DL, Jongens TA: Genetic characterization of the 44D-45B region of the *Drosophila melanogaster* genome based on an F2 lethal screen. *Mol Gen Genet* 2000; 263:137-43
31. Mohr SE, Boswell RE: Genetic analysis of *Drosophila melanogaster* polytene chromosome region 44D-45F: Loci required for viability and fertility. *Genetics* 2002; 160:1503-10
32. Yang Z, Harrison SM, Steele DS: ATP-dependent effects of halothane on SR  $Ca^{2+}$  regulation in permeabilized atrial myocytes. *Cardiovasc Res* 2005; 65:167-76
33. Mody I, Tanelian DL, MacIver MB: Halothane enhances tonic neuronal inhibition by elevating intracellular calcium. *Brain Res* 1991; 538:319-23
34. Gomez RS, Guatimosim C, Barbosa J Jr, Massensini AR, Gomez MV, Prado MA: Halothane-induced intracellular calcium release in cholinergic cells. *Brain Res* 2001; 921:106-14
35. Kushnir A, Betzenhauser MJ, Marks AR: Ryanodine receptor studies using genetically engineered mice. *FEBS Lett* 2010; 584:1956-65
36. Diaz-Sylvester PL, Porta M, Copello JA: Halothane modulation of skeletal muscle ryanodine receptors: Dependence on  $Ca^{2+}$ ,  $Mg^{2+}$ , and ATP. *Am J Physiol Cell Physiol* 2008; 294:C1103-12
37. Trapp S, Lückermann M, Kaila K, Ballanyi K: Acidosis of hippocampal neurones mediated by a plasmalemmal  $Ca^{2+}/H^{+}$  pump. *Neuroreport* 1996; 7:2000-4
38. Enyedi P, Czirkák G: Molecular background of leak  $K^{+}$  currents: Two-pore domain potassium channels. *Physiol Rev* 2010; 90:559-605
39. Brosnan RJ, Eger EI II, Laster MJ, Sonner JM: Anesthetic properties of carbon dioxide in the rat. *Anesth Analg* 2007; 105:103-6
40. Wei H: The role of calcium dysregulation in anesthetic-mediated neurotoxicity. *Anesth Analg* 2011; 113:972-4
41. Berge KE, Haugaa KH, Früh A, Anfinson OG, Gjesdal K, Siem G, Oyen N, Greve G, Carlsson A, Rognum TO, Hallerud M, Kongsgård E, Amlie JP, Leren TP: Molecular genetic analysis of long QT syndrome in Norway indicating a high prevalence of heterozygous mutation carriers. *Scand J Clin Lab Invest* 2008; 68:362-8
42. Kochs E, Hoffman WE, Roewer N, Schulte am Esch J: Alterations in brain electrical activity may indicate the onset of malignant hyperthermia in swine. *ANESTHESIOLOGY* 1990; 73:1236-42